



# Initial Conditions for Carbon-13 MAS NMR 1D Exchange Involving Chemically Equivalent and Inequivalent Nuclei

P. Tekely,<sup>\*,1</sup> D. Reichert,<sup>†</sup> H. Zimmermann,<sup>‡</sup> and Z. Luz<sup>§</sup>

<sup>\*</sup>Laboratoire de Méthodologie RMN, UPRESA CNRS 7042, Université Henri Poincaré, Nancy 1, 54506 Vandoeuvre-lès-Nancy, France; <sup>†</sup>Fachbereich Physik, Martin-Luther-Universität Halle-Wittenberg, 06108 Halle, Germany; <sup>‡</sup>AG Moleküllkristalle, Max-Planck-Institut für Medizinische Forschung, 6900 Heidelberg, Germany; and <sup>§</sup>Chemical Physics Department, Weizmann Institute of Science, Rehovot, 76100, Israel

Received January 12, 2000; revised March 28, 2000

A major problem in dynamic 1D <sup>13</sup>C MAS NMR concerns the exchange between magnetically inequivalent, but chemically equivalent sites, whose signals are not resolved in the regular 1D spectrum. This difficulty may be overcome by properly preparing the initial nonequilibrium state of the spin system in the exchange experiments. In the present paper we discuss the advantages and limitations of several such experiments already in use and propose a new sequence, which we term SELDOM-ODESSA. Unlike the other 1D-exchange methods, this experiment yields pure absorption spectra that can more readily be analyzed quantitatively. The experiment is a hybrid comprising a SELDOM sequence, for selective excitation of one of the spinning sideband manifolds in the spectrum, followed by the ODESSA sequence, which induces alternate polarization in the excited sideband manifold. The evolution of the spectrum following this sequence provides information on both the exchange between congruent sites belonging to the same group of equivalent nuclei, and the exchange between inequivalent sites. Results are presented for a tropolone sample specifically enriched in carbon-13 at the carbonyl and hydroxyl sites. The dominant exchange mechanism in this sample involves spin diffusion. The various spin exchange processes in this sample, in the presence and absence of proton decoupling during the mixing time, are measured and discussed. © 2000 Academic Press

**Key Words:** magnetization transfer; spin diffusion; SELDOM; ODESSA; tropolone.

## INTRODUCTION

Modern solid-state NMR techniques, such as one- and two-dimensional MAS experiments, serve as extremely powerful tools for the investigation of dynamic processes in solids (1, 2). Magnetization transfer methods are especially suited to the investigation of slow processes whose rates are of the order of, or slower than, the longitudinal relaxation times. The interpretation of such results in terms of molecular rotations or chemical transformation is, however, often hampered by spin diffusion, which has similar effects on the NMR spectra, as do real exchange processes (3). This effect, which depends on the

internuclear dipolar interactions, is often encountered in carbon-13 NMR, in particular of enriched samples. In fact, this effect can be turned to an advantage and is currently extensively used for structural studies in a variety of systems, including molecular crystals, amorphous materials, and biopolymers (4–12).

For the discussion of MAS exchange experiments in molecular crystals it is convenient to distinguish between the following three cases. (i) exchange between magnetically equivalent nuclei, i.e., nuclei related to each other by translation or inversion; (ii) exchange between congruent nuclei, i.e., nuclei that are related by other than the above symmetries. The principal values of their chemical shift (CS) tensors are identical, but their principal axes (PAS) are not, although they are related by the crystal symmetry; (iii) exchange between inequivalent nuclei, which have different CS tensors. Spin exchange between magnetically equivalent nuclei does usually not affect the MAS spectra, while the other two types of exchange processes can readily be distinguished from the nature of the cross-peaks between the spinning sidebands (ssb) in the spectra of rotor-synchronized 2D-exchange experiments (13–15). Thus, exchange between congruent nuclei (type ii) shows up as auto cross-peaks (i.e., cross-peaks between ssb belonging to the same manifold), while exchange between inequivalent nuclei (type iii) is manifested in the appearance of hetero cross-peaks linking ssb belonging to different manifolds.

Two-dimensional-exchange experiments are often very time-consuming. It is therefore desirable to look for alternative 1D methods. In fact, the standard magnetization transfer (MT) experiments (16, 17) are the methods of choice for studying exchange between inequivalent nuclei, providing the same type of information as the hetero cross peaks in 2D-exchange spectroscopy (18). The measurement of exchange between congruent nuclei, by 1D experiments, is subtler. Two such 1D methods were proposed. One involves a TOSS sequence and the monitoring of the ssb as they are reintroduced by the exchange, EIS, exchange induced ssb (19). More recently we have introduced an alternative 1D method (20), which we termed ODESSA, for one-dimensional exchange spectroscopy by

<sup>1</sup> To whom correspondence should be addressed. E-mail: [pt@meth-rmn.u-nancy.fr](mailto:pt@meth-rmn.u-nancy.fr).



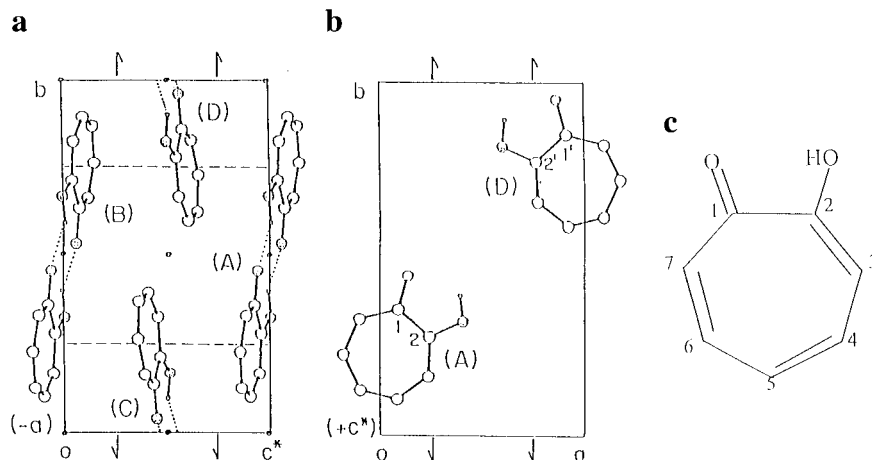


**FIG. 1.** Crystal and molecular structure of tropolone. (a) Projection down the  $a$  axis. (b) Projection down the  $c^*$  axis (only the A and D molecules are shown). (c) Structural formula and numbering system used.

sidebands alternation. The method is simple to apply when the spectrum consists of a single ssb manifold due to a number of interchanging congruent sites. However, the method results in phase distorted spectra when the spin system consists of several inequivalent groups of nuclei. In a later version of the ODESSA method, which we termed time reverse ODESSA (or tr-ODESSA) (21), the phase twist problem was eliminated for cases when the exchange involves only congruent nuclei, although it reappears when the exchange also involves inequivalent nuclei. A comparative study of the 2D-exchange, EIS, and ODESSA methods was recently published (22).

In the present paper we introduce yet another modification of the original ODESSA method, which eliminates the phase twist even in the presence of exchange between inequivalent nuclei. To do so we apply a selective excitation by a SELDOM pulse train (23) prior to the start of the ODESSA sequence, so that at the beginning of the mixing time only one ssb manifold is excited. During the mixing time, exchange between congruent, as well as between inequivalent, nuclei results in changes in the ssb intensities, all having the same phase as that of the originally excited ssb manifold. We demonstrate the use of this Sel-ODESSA method on a sample of carbon-13 enriched tropolone and compare its performance with several of the other 1D-exchange methods mentioned above.

### THE MODEL COMPOUND—CARBON-13 ENRICHED TROPOLONE

As a model compound we chose a tropolone sample selectively enriched with carbon-13 in the carbonyl (1) or the hydroxyl (2) positions (Fig. 1c). The synthesis of the compound (24) was such that 25% of the molecules were enriched in position 1 and another 25% were enriched in position 2, so that no doubly labeled molecules, other than those due to the natural isotopic abundance, are present. The  $T_1$  of the car-

bon-13 nuclei in this sample at room temperature is 90 s. Tropolone crystallizes in the monoclinic  $P2_1/c$  space group (25), with two centrosymmetric dimers per unit cell (Figs. 1a and 1b). The two molecules within a dimer are completely equivalent, because they are related by inversion symmetry, while the two dimers in the unit cell (e.g., A and D) are related by the monoclinic symmetry and are therefore congruent. Likewise, carbons 1 and 1' (Fig. 1b) are congruent as are carbons 2 and 2', but carbons 1(1') and 2(2') are, of course, inequivalent.

In the enriched sample enhanced spin diffusion results in fast spin exchange between all types of carbons (24, 26). Neglecting the naturally abundant carbon-13 nuclei, the  $^{13}\text{C}$  MAS spectrum of this sample exhibits two ssb manifolds due to carbons 1(1') and 2(2'). Such a spectrum, recorded by the standard CPMAS method (Fig. 2a), is shown in Fig. 3a. To obtain information on spin exchange between carbons 1 and 2, normal MT methods can be used; however, to measure the spin exchange between congruent pairs, ODESSA (or EIS) -type experiments must be performed. For the analysis of the results, we shall use the chemical shift tensors as derived in Ref. (26) (see Table 1).

For the calculation of the evolution of spectra during the mixing time due to exchange, we shall need the elements of the population matrix,  $P_{kl}$ ,

$$P_{kl}(\tau_m) = [\exp(K\tau_m)]_{kl} P_l(0), \quad [1]$$

defined as the fractional population of those nuclei that at the beginning of the mixing time were at site  $l$  and at its end in site  $k$ . The  $P_l(0)$  are the initial populations of sites  $l$ , and  $K$  is the exchange matrix. Considering for the moment just a single unit cell in the tropolone crystal,  $K$  acquires the form,

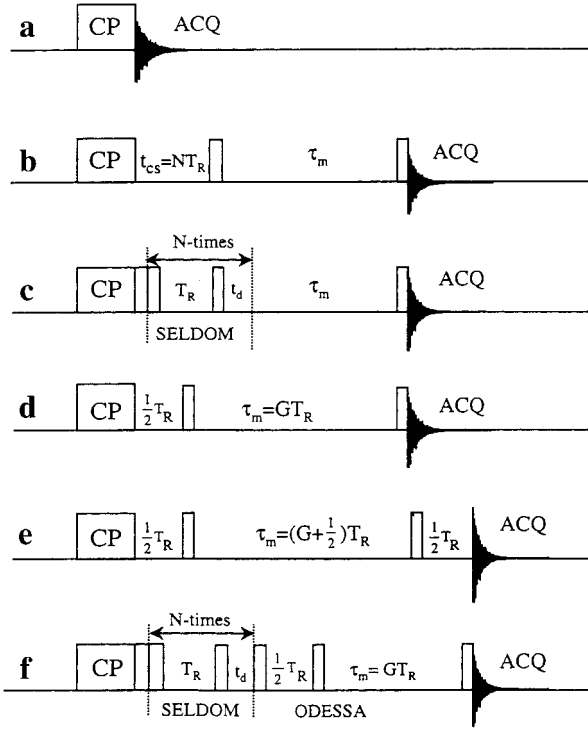


**FIG. 2.** Pulse sequences for MAS 1D-exchange experiments with different preparations of the initial nonequilibrium  $z$ -magnetization (only the  $X$  channel is depicted). (a) Regular CP-MAS. (b) Magnetization transfer (MT) for two inequivalent sites. The evolution period,  $t_{cs}$ , is adjusted to bring the two magnetizations into antiphase and at the same time to be an integer number of rotation periods. (c) Sel-MT, with selective excitation of a single ssb manifold. (d) ODESSA pulse sequence. The preparation period is half a rotation and the mixing time is an integer number of rotations. (e) Time reverse ODESSA (tr-ODESSA). The preparation period is half a rotation period, the mixing time is an odd number of half rotation periods, and the acquisition starts half a rotation after the read-out pulse. (f) SELDOM-ODESSA (Sel-ODESSA): a hybrid 1D-exchange experiment consisting of a SELDOM pulse train followed by the ODESSA sequence.

$$K = \begin{pmatrix} -k & k_{11'} & k_{12} & k_{12'} \\ k_{1'1} & -k & k_{1'2} & k_{1'2'} \\ k_{21} & k_{21'} & -k & k_{22'} \\ k_{2'1} & k_{2'1'} & k_{2'2} & -k \end{pmatrix}, \quad [2]$$

where  $k = k_{1'1} + k_{21} + k_{2'1}$  and  $k_{ik} = k_{ki}$ . Also, by symmetry  $k_{12} = k_{1'2'}$ , and we shall assume that  $k_{11'} = k_{22'}$ . We are thus left with only three independent rate constants,  $k_{11'}$ ,  $k_{12}$ , and  $k_{12'}$ . Under these circumstances, the conditional probabilities in Eq. [1] become

$$\exp[K(\tau_m)] = \begin{pmatrix} a & b & c & d \\ b & a & d & c \\ c & d & a & b \\ d & c & b & a \end{pmatrix}, \quad [3]$$

where

$$a = 1 + A + B + C, \quad b = 1 - A - B + C,$$

$$c = 1 - A + B - C, \quad d = 1 + A - B - C,$$

and

$$A = \exp[-2(k_{11'} + k_{12})\tau_m],$$

$$B = \exp[-2(k_{12} + k_{12'})\tau_m],$$

$$C = \exp[-2(k_{12'} + k_{11'})\tau_m].$$

When the spin exchange is governed by spin diffusion it involves all pairs of nuclei in the lattice with a distribution of rate constants, depending on their mutual dipolar interactions. An approximate expression for the rate constant of the spin-diffusion process has the form  $k_{ij} = d/r_{ij}^6$ , where  $r_{ij}$  is the internuclear distances and  $d$  is a constant depending on the nuclear magnetogyric ratio and on an ill-defined spectral overlap function. Using the tropolone lattice as determined by X-ray crystallography (25) with  $6 \times 6 \times 6$  unit cells and fixed  $d$  values ( $1.145 \times 10^4 \text{ \AA}^6 \text{ s}^{-1}$  for  $i, j = 1, 1'$  and  $2, 2'$ . and  $0.716 \times 10^4 \text{ \AA}^6 \text{ s}^{-1}$  for  $i, j = 1, 2$  and  $1, 2'$ , etc.) we computed the time dependence of the following populations:  $P_{11'}$ ,  $P_{22'}$ , and the sum of  $P_{12}$  and  $P_{12'}$ . The computation procedure is described in Ref. (26) and the results (open circles) are plotted in Fig. 4. The main points to notice are, first, that the evolution of the  $P_{ij}$ 's is not exponential. This is not so readily seen in the linear-log plots of Fig. 4, but becomes quite evident in log-linear plots (26). We shall, nevertheless, use the former way of presenting results because it makes it easier to discriminate between dynamic processes of different time scales. Second, the curves for  $P_{11'}$  and  $P_{22'}$  are nearly the same, thus justifying the assumption made above that  $k_{11'} = k_{22'}$ .

Decay functions due to a distribution of rate constants are often expressed in terms of stretched exponentials (27),

$$\exp(-kt^\beta),$$

where  $\beta$  is a measure of the distribution. We have accordingly fitted the results of Fig. 4 to equations of the form  $A[1 - \exp(-k\tau_m^\beta)]$ . The results are drawn as solid curves in the figure. The fit to the experimental points is quite satisfactory and yields  $\beta$  values in the range of 0.62 to 0.74. In the analysis of the experimental data we shall still use Eqs. [3], but rather than simple exponential functions we shall fit them to stretched exponents with fixed  $\beta = 0.68$ . We wish to emphasize that this is still an approximation, but indirectly accounts for the distribution in the rate constants and considerably simplifies the analysis.

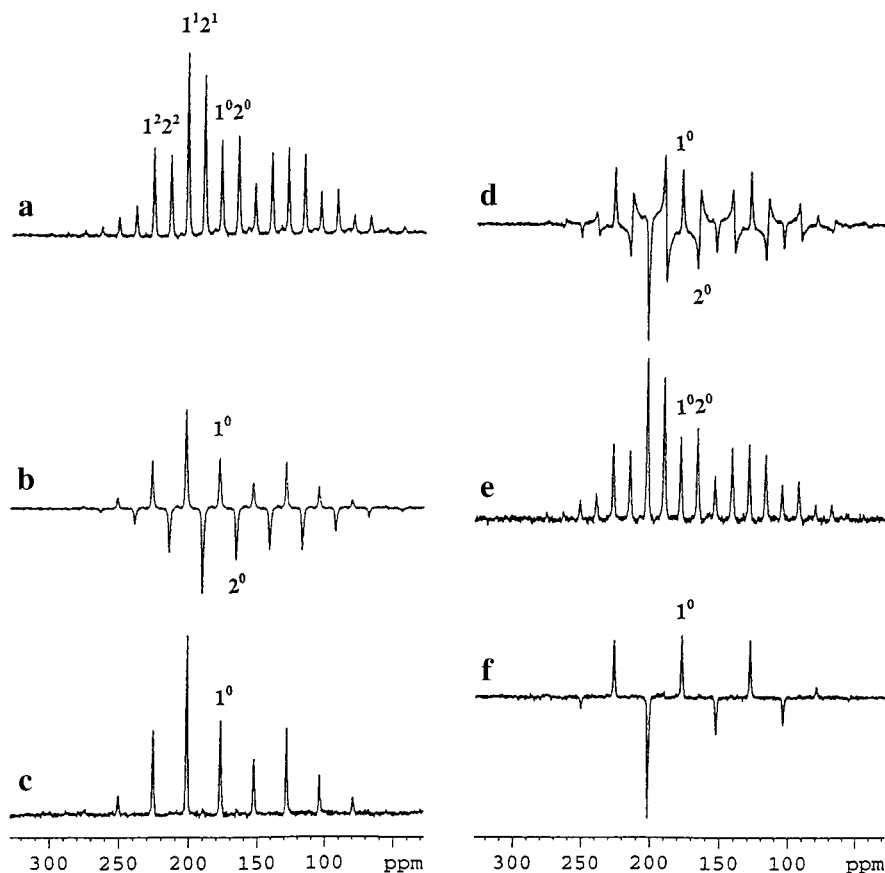


**FIG. 3.** Carbon-13 spectra of the tropolone sample at a spinning rate of 1.84 kHz for different pulse sequences. The cross-polarization contact time was 1 ms and in the 1D-exchange experiments the mixing time was the shortest possible (one rotation period, except for tr-ODESSA where it was half a rotation). (a) Standard CP-MAS spectrum. The centerbands ( $N = 0$ ) and the  $N = 1, 2$  ssb of carbons 1 and 2 are indicated. (b) Spectrum obtained with the MT sequence (Fig. 2b) with selective inversion of the ssb manifold of carbon 2. (c) Spectrum obtained with the MT sequence of Fig. 2c by selectively exciting the ssb manifold of carbon 1, using a modified SELDOM pulse train, employing  $135^\circ$  (rather than the usual  $90^\circ$ ) pulses. (d) ODESSA spectrum, obtained with the pulse sequence of Fig. 2d. (e) tr-ODESSA spectrum obtained with the pulse sequence of Fig. 2e. (f) Spectrum obtained using the Sel-ODESSA sequence of Fig. 2f, by selective excitation of the ssb of carbon 1.

## EXPERIMENTAL

The MAS NMR measurements were carried out on a Bruker DSX300 spectrometer operating at a carbon-13 frequency of 75.5 MHz. All measurements were performed at room temperature ( $22^\circ\text{C}$ ) on the enriched tropolone sample described in the previous section. Its synthesis has been described in Ref. (24).

**TABLE 1**  
**Chemical Shift Parameters for Carbons 1 and 2 of Tropolone**  
**(from Ref. 26)<sup>a</sup>**

	$\sigma_{\text{iso}}$	$\sigma_{xx}$	$\sigma_{yy}$	$\sigma_{zz}$
Carbon 1	177.8	66	32	-98
Carbon 2	165.8	76	18	-94

<sup>a</sup> The  $x$  axes are perpendicular to the molecular plane. The  $y$  axis of carbon 1 is  $9^\circ$  off the C=O bond while that of carbon 2 is off from the C2-C3 bond by  $10^\circ$ .

Rotor synchronization was affected as described in Ref. (20). Typical experimental conditions were carbon-13  $\pi/2$  pulse width, 4  $\mu\text{s}$ ; proton  $\pi/2$  pulse width, 4.2  $\mu\text{s}$ ; CP contact time, 1 ms; recycle time 10 s. The number of accumulations ranged between 16 and 80, depending on the type of experiment.

## PULSE SEQUENCES AND BASIC EQUATIONS

### (a) MT Sequences

Figure 2 shows different pulse sequences for 1D MAS exchange methods. Sequences 2b and 2c are normal MT experiments, while the rest are of the ODESSA type. The various sequences differ in the way the spin systems are prepared before the mixing time. These initial states are visualized in the spectra of Fig. 3, which were recorded after a “zero” mixing time (in practice one, or one-half, rotation period).

Figure 2b shows a sequence often used to measure exchange between two inequivalent sites (16, 17). The fixed delay pe-

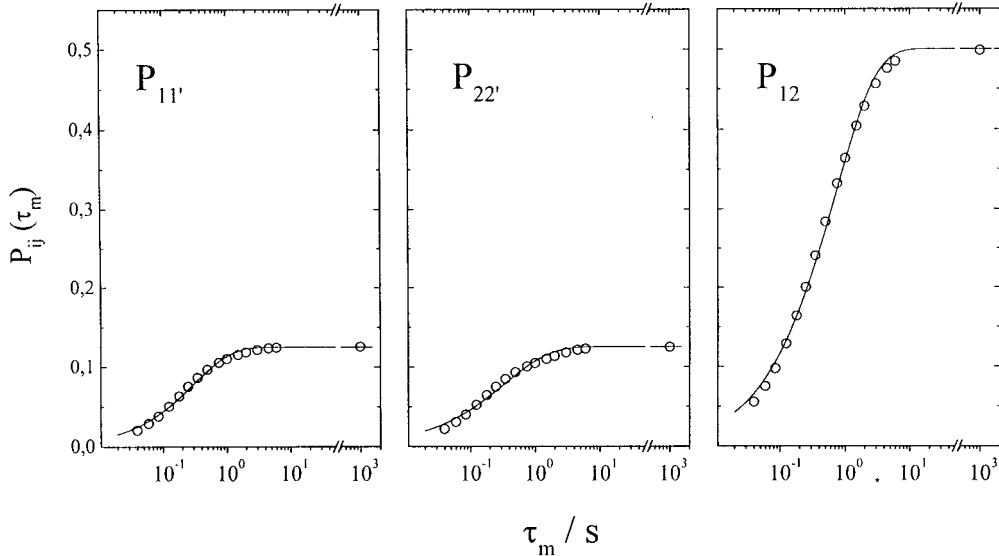


**FIG. 4.** Plots of the fractional populations,  $P_{ij}(\tau_m)$ , of nuclei which initially occupied site  $j$  and at time  $\tau_m$  site  $i$ , for carbons 1 and 2 in crystalline tropolone.  $P_{12}$  in this figure is the sum of  $P_{12}$  and  $P_{12'}$ . The spin exchange mechanism was assumed to be spin diffusion. The calculations were performed as described in Ref. (26). A lattice of  $6 \times 6 \times 6$  unit cells was used for a sample enriched to 25% in carbon-13 at positions 1 and 2. The open circles are results of the calculations and the solid lines are best fits to stretched exponentials functions of the form  $A[1 - \exp(-k_{ij}\tau_m^\beta)]$ .

riod,  $t_{cs}$ , during the preparation stage is adjusted so that after the following  $\pi/2$  pulse one magnetization is selectively inverted relative to the other. At the same time it is also necessary to ensure that  $t_{cs}$  equals an integer number of rotation periods (Fig. 3b). The latter condition is essential to achieve an initial state of full difference magnetization between the two ssb manifolds. The approach to equilibrium as a result of spin exchange and relaxation processes is then readily analyzed in terms of standard kinetic equations. As explained above, for processes governed by spin diffusion we shall use stretched exponents, so that

$$\frac{[I^1(\tau_m) - I^2(\tau_m)] - [I_{eq}^1 - I_{eq}^2]}{[I^1(0) - I^2(0)] - [I_{eq}^1 - I_{eq}^2]} = \exp[-(k_{12} + k_{21})\tau_m^\beta] \exp(-\tau_m/T_1), \quad [4]$$

where the  $I^i$ 's are the ssb intensities (either of a selected one or a sum over several).

When there are more than just two types of inequivalent nuclei in the system, alternative sequences must be sought to selectively excite one ssb manifold. Such a sequence is shown in Fig. 2c, where the preparation period includes a SELDOM pulse train (23), which saturates all ssb manifolds but one (Fig. 3c). Since, however, we wished to compare spectra recorded under the same MAS frequency, we could not, in the present case, use the normal SELDOM sequence (a train of  $\pm 90^\circ$  pulses). Such a pulse train would lead to an antiphase alignment of the two manifolds and not to selective saturation. Instead, we used a train of  $\pm 135^\circ$  pulses. It is easy to see that

such a sequence would leave the nonresonant ssb manifolds in the  $x - y$  plane during the  $t_d$  delay and eventually to their complete saturation.

#### (b) ODESSA-type Sequences

Sequences 2b and 2c are not suitable for studying exchange between congruent sites. For such measurements, an ODESSA type sequence (20, 21) must be used. The original ODESSA sequence is the same as for the rotor-synchronized MAS 2D-exchange experiment (13, 14), except that the evolution time is fixed at  $T_R/2$  (Fig. 2d). The mixing time is adjusted to an integer number of rotation periods,  $\tau_m = GT_R$ , and the phase cycle is adjusted so that the anti-echo combination is stored in the receiver (15). This sequence leads to alternate, even-odd polarization of the ssb (20). Since different congruent sites contribute differently to the various ssb (28), spin exchange will result in redistribution of the polarization and to a corresponding change in the sideband intensities.

Equations describing the evolution of the peak intensities as a function of the mixing time in the ODESSA experiment were derived in Ref. (20). Here we shall only give the final equations for the anti-echo time-domain signal,

$$S^+(t, \tau_m) = \sum_a \exp(i\omega_{iso}^a T_R/2) \sum_N I_N^a(\tau_m) \times \exp[i(\omega_{iso}^a + N\omega_R)t], \quad [5]$$

where the sideband intensities of the  $a$ th manifold  $I_N^a(\tau_m)$ , are given by



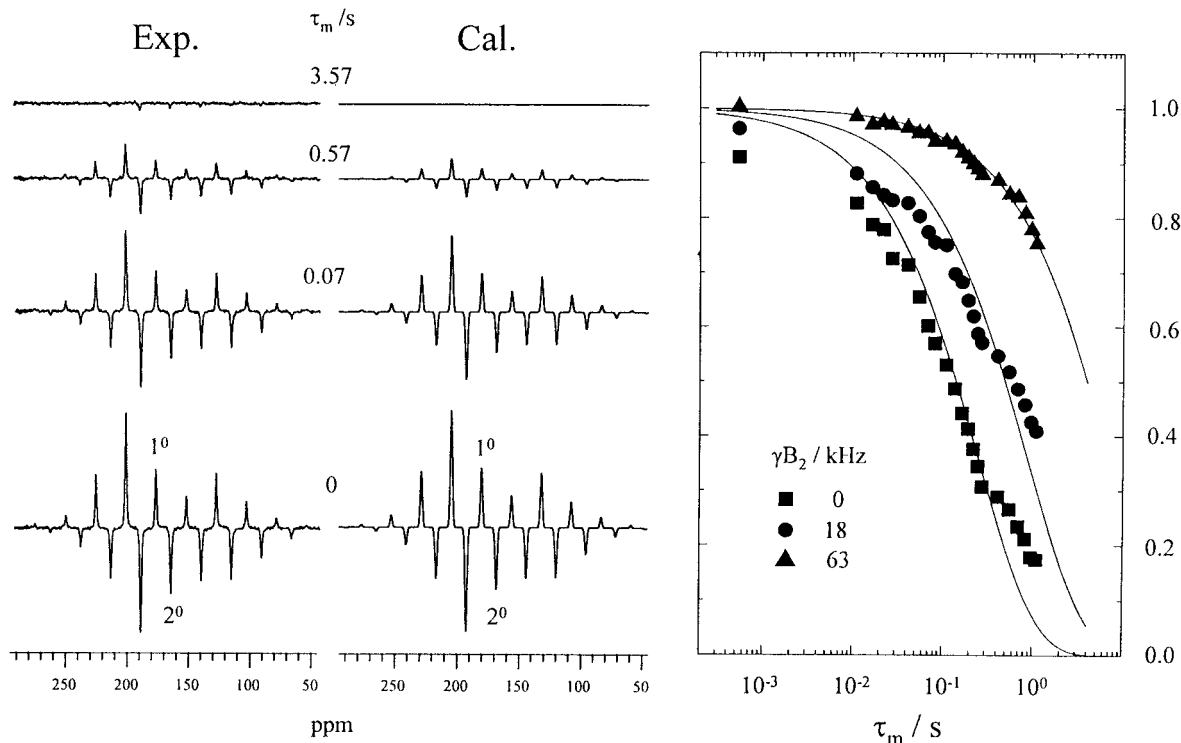


**FIG. 5.** Experimental carbon-13 MT spectra (Fig. 2b) of the tropolone sample recorded for different mixing times as indicated ( $\nu_R = 1.84$  kHz,  $\gamma B_2 = 0$ , total number of scans, 32). Center: Corresponding simulated spectra using Eq. [4] and parameters given in Tables 1 and 2. Right: Intensity plots (left-hand side of Eq. [4]), for different proton decoupling powers  $\gamma B_2$  during the mixing time. The intensities are sums of the three most intense ssb ( $N = 0, 1, 2$ ).

$$I_N^a(\tau_m) = \left[ \sum'_{ai,bj} P_{ai,bj}(\tau_m) \sum_M (-)^M I_{MN}^{ai,bj} \right] \exp(-\tau_m/T_1), \quad [6]$$

where  $\Sigma'$  means summation over all  $bj$  ( $b \neq a$ ) and all  $i$  in  $a$  (but not over  $a$ ). In these equations  $\omega_{iso}^a$  is the isotropic CS of all the congruent sites of type  $a$ , and  $N, M$  label the ssb, with 0 corresponding to the centerband. The indices  $a, b$ , label the various groups of equivalent nuclei and the indices  $i, j$  label the different congruent sites within each group. The terms  $I_{MN}^{ai,bj}$  are the normalized cross-peak intensities in rotor-synchronized MAS 2D-exchange experiment. Their definition in terms of the CS tensors of the interchanging sites is given in Ref. (26). In Eq. [6], the summation index  $ai(bj)$  corresponds to all congruent sites  $i(j)$  in  $a(b)$ .

The normal ODESSA method works well for a single group of equivalent nuclei. When several inequivalent groups of nuclei are present, each ssb manifold acquires a different phase factor of  $\omega_{iso}^a T_R/2$  (see Eq. [5]), which cannot be cancelled simultaneously for all manifolds. Figure 3d shows a spectrum of the tropolone sample recorded by this sequence. The phases of the ssb of carbon-1 have been adjusted to pure absorption, consequently those of carbon-2 are twisted.

The problem was partially resolved by the tr-ODESSA sequence (21) shown in Fig. 2e. It differs from the normal ODESSA in that the mixing time is adjusted to the last half of

an odd integer number of rotation periods,  $\tau_m = (2G + 1)T_R/2$ , the acquisition starts  $T_R/2$  after the read-out pulse and the phase cycle ensures that the echo (rather than the anti-echo) signal is stored in the receiver. The resulting signal then has the form (21)

$$S^-(t, \tau_m) = \sum_a \sum_N (-)^N J_N^a(\tau_m) \exp[i(\omega_{iso}^a + N\omega_R)t], \quad [7]$$

where, however, the sideband intensities,  $J_N^a$ , are now defined as

$$J_N^a(\tau_m) = \sum'_{ai,bj} P_{ai,bj}(\tau_m) \exp[i(\omega_{iso}^a - \omega_{iso}^b)T_R/2] \times \sum_M (-)^M I_{NM}^{ai,bj}(\tau_m) \exp(-\tau_m/T_1). \quad [8]$$

Equation [8] differs from that for the normal ODESSA (Eq. [5]) in two respects. First, for exchange involving only congruent nuclei within the same symmetry type, there is no phase twist. Second, when  $\tau_m = 0$  the observed spectrum is identical to that of the normal MAS with all peaks “positive” (see Fig. 3e), rather than alternating as in normal ODESSA. The resemblance of the spectrum to that of normal MAS is a bit mis-

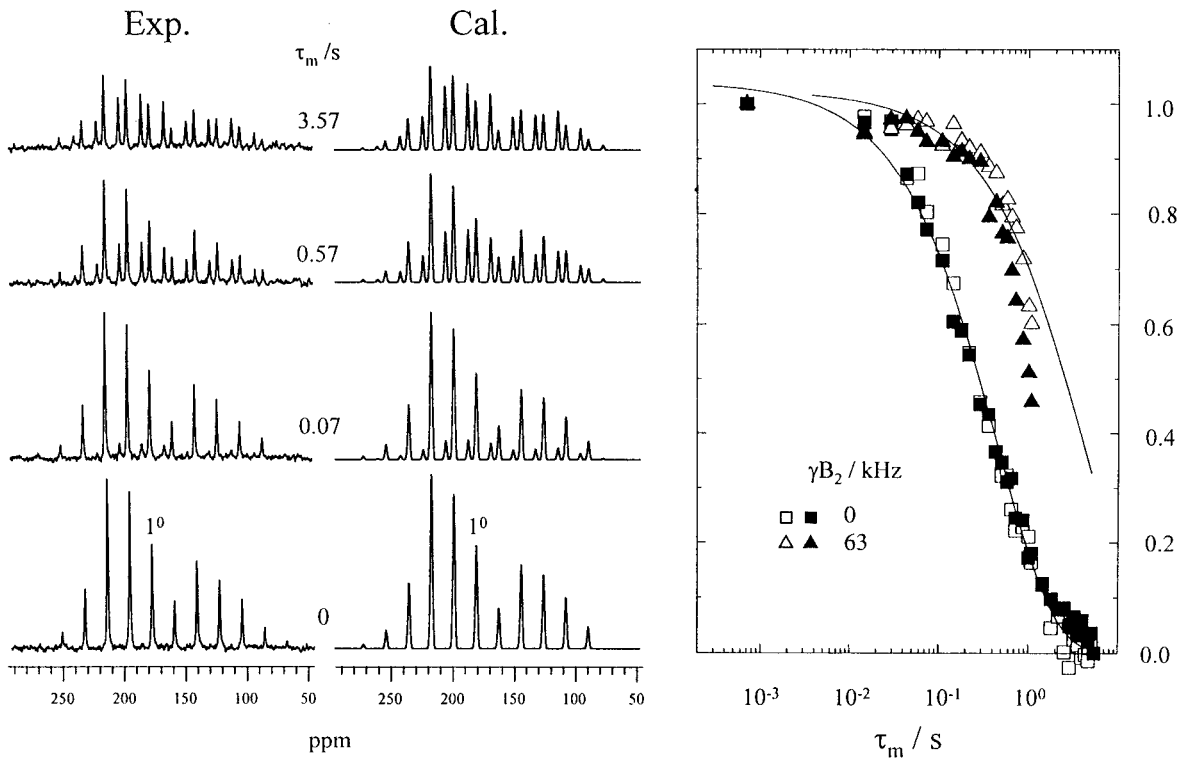


**FIG. 6.** Left: Sel-MT (Fig. 2c) spectra of the tropolone sample, for the indicated mixing times ( $\nu_R = 1.40$  kHz,  $\gamma B_2 = 0$ , total number of scans, 64). The selective excitation of carbon 1 was achieved by a rotor-synchronized SELDOM train of twenty  $90^\circ$  pulses with  $t_d = 1$  ms. Center: Corresponding simulated spectra using Eq. [4] and parameters given in Tables 1 and 2. Right: Intensity plots (left-hand side of Eq. [4]) as function of the mixing time for different decoupling powers. Open and closed symbols correspond to excitation of carbon 1 and 2, respectively. The intensities are sums of the  $N = 0, 1$ , and 2 ssb.

leading. In reality the alternate polarization of the ssb is also present in the tr-ODESSA throughout the mixing time as in normal ODESSA, but is canceled by the  $T_R/2$  delay that follows the detection pulse. When exchange between inequivalent nuclei ( $a$  and  $b$ ) takes place a phase twist proportional to  $(\omega_{\text{iso}}^a - \omega_{\text{iso}}^b)T_R/2$  will show up. It can, in fact, be phased symmetrically for both manifolds and used for kinetic studies by eye fitting with simulated spectra (see below). However, for quantitative analysis of complex situations one desires to work with pure absorption spectra.

**TABLE 2**  
**Best-Fit Rate Constants for the Spin-Diffusion Processes in the Enriched Tropolone Sample**

	$\nu_R/\text{kHz}$	$\gamma B_2/\text{kHz}$	$k_{11}, k_{22}/\text{s}^{-1}$	$k_{12}, k_{12}/\text{s}^{-1}$
MT	1.84	0	0.86	1.0
		18		0.44
		63		0.11
		0		0.38
Sel-MT	1.4	0	3.0	0.71
		63		0.21
Sel-ODESSA	1.4	0	0.86	0.86
		63		0.21

For that purpose we propose another modification of the ODESSA method which does exactly that, i.e., it results in undistorted ODESSA spectra even in situations where the exchange involves inequivalent sites. To do so we precede the ODESSA sequence with a selective excitation so that at the beginning of the mixing time only one ssb manifold is excited. A pulse sequence that does the trick well is shown in Fig. 2f. It consists of a SELDOM pulse train, followed by the normal ODESSA experiment. An example of a spectrum acquired by this Sel-ODESSA sequence is shown in Fig. 3f. This sequence ensures that only the selected group of equivalent nuclei acquires a phase delay during the ODESSA preparation period, so that the equation for the Sel-ODESSA signal becomes

$$S^+(t, \tau_m) = \exp(i\omega_{\text{iso}}^a T_R/2) \sum_b \sum_N I_N^b(\tau_m) \times \exp[i(\omega_{\text{iso}}^b + N\omega_R)t]. \quad [9]$$

As may be seen from this equation, all the ssb manifolds acquire the same constant phase even when exchange between inequivalent nuclei takes place. The main disadvantage of the method is the diminished signal intensity, due to the selective excitation of the spectrum and losses inherent to the SELDOM sequence.

In the next section we apply the various sequences to the enriched tropolone sample. As discussed above, this sample exhibits exchange both between congruent and between inequivalent sites, thus allowing us to evaluate the merits and limitations of the various methods.

## RESULTS AND DISCUSSION

### (a) MT Experiments

The left-hand side of Fig. 5 shows the results of the MT experiments on the enriched tropolone sample recorded with pulse sequence b of Fig. 2. In this experiment the polarization of carbon 2 ( $2'$ ) was initially inverted and the approach to equilibrium as a function of the mixing time was monitored. Simulated spectra calculated using Eq. [4] are shown in the center column. Relevant plots are given on the right-hand side. They include results from three exchange experiments recorded in the absence of proton decoupling during the mixing time, intermediate decoupling, and maximum decoupling power tolerable by our probe, respectively. Similar results for the Sel-MT experiment (Fig. 2c) are shown in Fig. 6. The solid lines in the diagrams of Figs. 5 and 6 were fitted to the experimental results using Eq. [4] and the resulting kinetic parameters are summarized in Table 2. We shall address these results in the last section of the paper. Regarding the sensitivity of the Sel-MT experiment, it is clear that for just two inequivalent sets of interchanging nuclei, Sel-MT has no advantage over normal MT. It may, however, be useful in more complex systems, where spectra simplification may be necessary.

### (b) ODESSA Experiments

To obtain information on the spin exchange between congruent pairs of carbons, it is necessary to perform ODESSA-type (or EIS) experiments. The normal ODESSA spectra (Fig. 3d) for spin systems with several ssb manifolds cannot, however, be simultaneously phased, even at  $\tau_m = 0$ . We, therefore, resort to tr-ODESSA (Fig. 2e). Spectra recorded with this sequence are shown in the left column of Fig. 7, with corresponding simulated traces (using Eq. [7]) on the right. Initially (short  $\tau_m$ 's) both manifolds are phased to pure absorption, but with increasing  $\tau_m$ , a phase twist, due to exchange between the inequivalent carbons 1 and 2, sets in. The fit between the experimental and simulated spectra is quite satisfactory and can be used for quantitative analysis of the spin exchange kinetics. However, in more general cases, where a large number of ssb manifolds is present, such an approach may be not easy to carry out in practice.

To eliminate the phase twist altogether we apply the Sel-ODESSA sequence depicted in Fig. 2f. Spectra recorded with this sequence, without and with proton decoupling during the mixing time, are shown in the first and third columns of Fig. 8, respectively. Well-phased spectra are obtained for all mixing times, starting at  $\tau_m = 0$ , where only one ssb manifold is

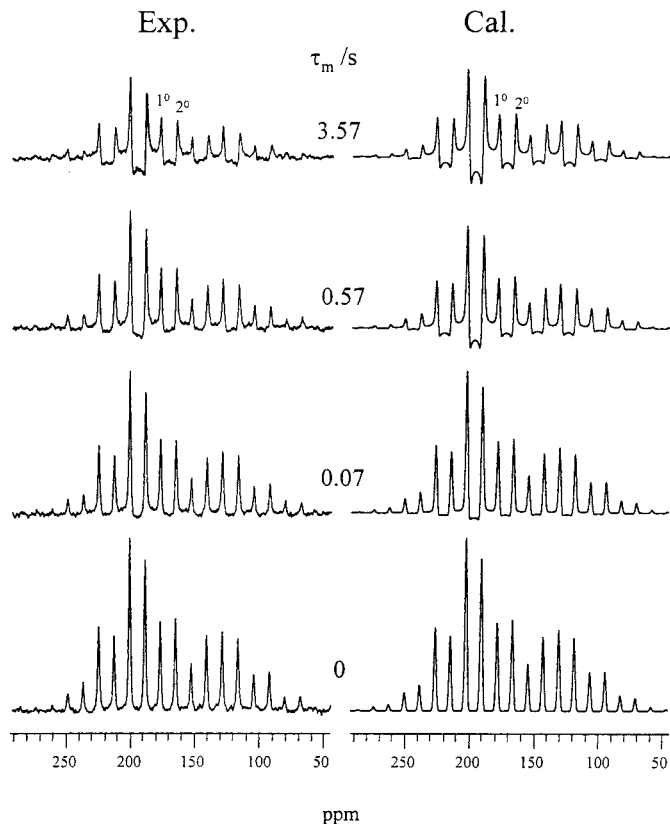


**FIG. 7.** Experimental (left) and simulated (right) tr-ODESSA (Fig. 2e) spectra of the tropolone sample ( $\nu_R = 1.40$  kHz,  $\gamma B_2 = 0$ , total number of scans, 32) for different mixing times. The simulated spectra were calculated from Eq. [7] with the parameters of Tables 1 and 2.

observed, up to large  $\tau_m$ 's, where the spectrum consists of two manifolds. The second and fourth columns show corresponding simulated traces and in Fig. 9 the normalized intensities for the  $N = 0, 1$ , and 2 ssb of both carbons are plotted. The solid lines in this figure are best-fit curves calculated using Eq. [9]. The resulting kinetic parameters are summarized in Table 2. Although the fit is not perfect, in particular the intensities of the peaks due to carbon 2 are smaller than expected from the simulations, the overall agreement is quite satisfactory. Especially pronounced is the effect of decoupling in hindering the spin exchange between inequivalent nuclei and at the same time enhancing the spin exchange between congruent sites.

## SUMMARY AND CONCLUSIONS

We have discussed several 1D MAS exchange experiments, with particular emphasis on spin exchange between congruent nuclei. For such measurements ODESSA-type experiments (or EIS) must be used. In the present work we introduced a new experiment, consisting of a hybrid of the SELDOM and the ODESSA sequences. Unlike in the earlier versions of the ODESSA method, the spectra resulting from this Sel-ODESSA



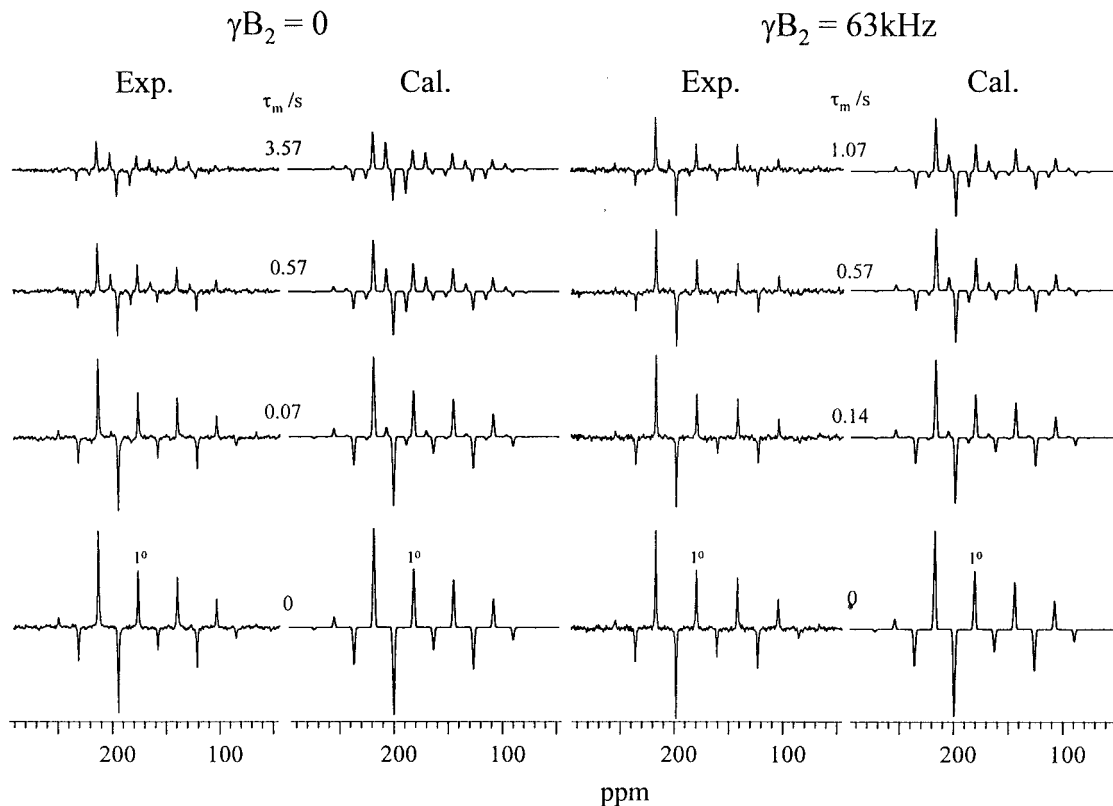


**FIG. 8.** Sel-ODESSA (Fig. 2f) spectra of the tropolone sample for different mixing times, without (left two columns) and with (right two columns) proton decoupling during the mixing time ( $\nu_R = 1.40$  kHz, total number of scans, 80). For each case the left column is experimental and the right one is calculated from Eq. [9] and parameters given in Tables 1 and 2.

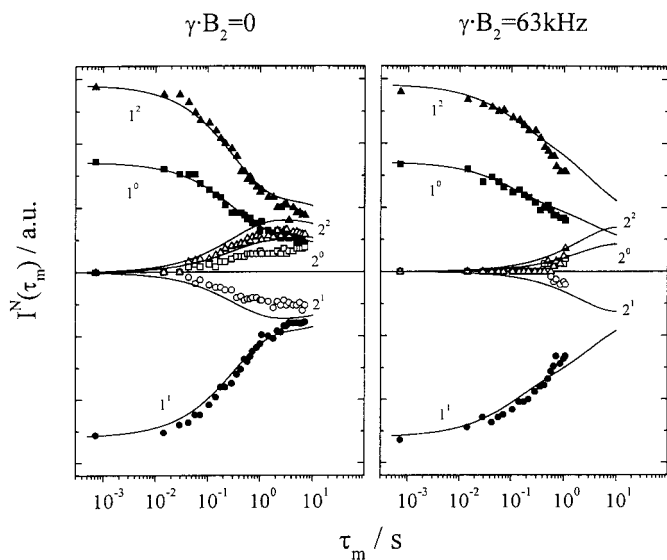


**FIG. 9.** Plots of the  $N = 0, \pm 1$  ssb of carbons 1 and 2 obtained by Sel-ODESSA experiments of the type shown in Fig. 8. Left: Without proton decoupling. Right: With proton decoupling during the mixing time. The solid curves are calculated from Eq. [9] with the rate constants shown in Table 2.

experiment can readily be phased to pure absorption for all mixing times. It is therefore more suitable for quantitative kinetic analysis. On the other hand, the method suffers from a reduced signal-to-noise ratio, since only one ssb manifold is excited and there is an additional loss in intensity due to transverse relaxation during the SELDOM sequence.

We have applied the various methods to measure the spin exchange rate in a tropolone sample specifically enriched in  $^{13}\text{C}$  in the carbonyl and hydroxyl positions. In this enriched sample the spin exchange is dominated by spin diffusion. Two such processes may be distinguished in tropolone, viz., spin exchange between the inequivalent carbons 1( $1'$ ) and 2( $2'$ ) and spin exchange between the congruent carbons 1( $2$ ) and  $1'$ ( $2'$ ). The enriched tropolone sample thus seems to provide an ideal system for comparing the various experimental methods. In practice, in the absence of proton decoupling, the results were not sensitive to the spin-diffusion rates between the congruent nuclei,  $k_{11'}$  and  $k_{22'}$ . This is partly due to the fact that the orientation differences between the CS tensors of carbons 1 and  $1'$  and between carbons 2 and  $2'$  are quite small (24, 26). Consequently, exchange between such pairs results in a small effect on the ssb intensities, which is difficult to detect in the presence of other similarly fast processes (exchange between inequivalent nuclei). This is particularly so because the com-

bined exchanges between the inequivalent nuclei,  $1 \rightarrow 2$  and  $2 \rightarrow 1'$ , is indirectly equivalent to  $1 \rightarrow 1'$ , thus masking the effect of the direct  $1 \rightarrow 1'$  process.

Referring to Table 2, several effects may be noted. In a simple-minded picture of proton-driven spin diffusion, the rate of the process appears to depend on the spectral overlap between the interchanging resonances (29). This overlap may be affected by external factors, such as proton decoupling during the mixing time or the sample-spinning rate. The results of Table 2 are consistent with this picture. In particular, there is a pronounced reduction in  $k_{12}$  with increasing the decoupling power, which clearly reflects the decrease in the spectral overlap between carbons 1 and 2. Likewise, there is a reduction in  $k_{12}$  with increasing the spinning rate (see the MT results in Table 2). The power of the Sel-ODESSA method is well demonstrated by the corresponding results for  $k_{11'}$ , which could only be obtained by this method. For this process, i.e., spin exchange between congruent nuclei, the effect of proton decoupling is opposite to that for exchange between inequivalent nuclei. Here the decoupling increases the "self-overlap" of the spectral lines and consequently leads to an acceleration of the spin-diffusion process, as indeed observed experimentally.

### ACKNOWLEDGMENTS

This work was supported by the German-Israel Foundation, G.I.F. Research Grant I-558-218.05/97, by the G.M.J. Schmidt Center on Supramolecular Architectures, the Deutsche Forschungsgemeinschaft (SFB 418), and the Fonds der Chemischen Industrie. We thank Dr. R. Poupko (Rehovot) and Prof. H. Schneider (Halle) for helpful discussion.

### REFERENCES

1. R. R. Ernst, G. Bodenhausen, and A. Wokaun, "Principles of Nuclear Magnetic Resonance in One and Two Dimensions," Clarendon Press, Oxford (1987).
2. K. Schmidt-Rohr and H. W. Spiess, "Multidimensional Solid-State NMR and Polymers," Academic Press, San Diego (1994).
3. B. H. Meier, Polarization transfer and spin diffusion in solid-state NMR, *Adv. Magn. Opt. Reson.* **18**, 1-116 (1994).
4. H. T. Edzes and J. P. C. Bernardis, Two-dimensional exchange NMR in static powders: Interchain  $^{13}\text{C}$  spin exchange in crystalline polyethylene, *J. Am. Chem. Soc.* **106**, 1515-1517 (1984).
5. M. Linder, P. M. Henrichs, J. M. Hewitt, and D. J. Massa, Use of carbon-carbon nuclear spin diffusion for the study of the miscibility of polymer blends, *J. Chem. Phys.* **82**, 1585-1589 (1985).
6. P. M. Henrichs, M. Linder, and J. M. Hewitt, Dynamics of the carbon-13 spin-exchange process in solids: A theoretical and experimental study, *J. Chem. Phys.* **85**, 7077-7086 (1985).
7. P. Caravatti, J. Dell, G. Bodenhausen, and R. R. Ernst, Direct evidence of microscopic homogeneity in disordered solids, *J. Am. Chem. Soc.* **104**, 5506-5507 (1982).
8. P. Robyr, B. H. Meier, and R. R. Ernst, Tensor correlation by 2D spin-diffusion powder NMR spectroscopy: Determination of the asymmetry of the hydrogen-bond potential in benzoic acid, *Chem. Phys. Lett.* **187**, 471-478 (1991).
9. P. Robyr, Z. Gan, and U. W. Suter, Local order between chain segments in the glassy polycarbonate of 2,2-bis(4-hydroxyphenyl) propane from  $^{13}\text{C}$  polarization-transfer NMR, *Macromolecules* **31**, 6199-6205 (1998).
10. H. Kaji and F. Horii, Analyses of the local order in poly(ethylene terephthalate) in the glassy state by two-dimensional solid-state  $^{13}\text{C}$  spin diffusion magnetic resonance spectroscopy, *J. Chem. Phys.* **109**, 4651-4658 (1998).
11. W. Heinen, C. B. Wenzel, C. H. Rosenmoeller, F. M. Mulder, M. Fokko, G. J. Boender, J. Lugtenburg, H. J. M. de Groot, M. van Duin, and B. Klumperman, Solid-state NMR study of miscibility and phase separation in blends and semi-interpenetrating networks of  $^{13}\text{C}$ -labeled poly(styrene-co-acrylonitrile) and poly(styrene-co-maleic anhydride), *Macromolecules* **31**, 7404-7412 (1998).
12. P. Tekely, M. J. Potrzebowski, Y. Dusaosoy, and Z. Luz, Measurements of spin diffusion and intermolecular distances between chemically equivalent nuclei in rotating solids, *Chem. Phys. Lett.* **291**, 471-479 (1998).
13. A. F. DeJong, A. P. M. Kentgens, and W. S. Veeman, Two-dimensional exchange NMR in rotating solids: A technique to study very slow molecular reorientations, *Chem. Phys. Lett.* **109**, 337-342 (1984).
14. A. Hagemeyer, K. Schmidt-Rohr, and H.W. Spiess, Two-dimensional magnetic resonance experiments for studying molecular order and dynamics in static and rotating solids, *Adv. Magn. Reson.* **13**, 85-130 (1989).
15. Z. Luz, H. W. Spiess, and J. J. Titman, Rotor synchronized MAS two-dimensional exchange NMR in solids. Principles and applications, *Isr. J. Chem.* **32**, 145-160 (1992).
16. N. M. Szeverenyi, A. Bax, and G. E. Maciel, Proton-exchange rates in solid tropolone as measured via carbon-13 CP/MAS NMR, *J. Am. Chem. Soc.* **105**, 2579-2582 (1983).
17. C. Connor, A. Naito, K. Takegoshi, and C. A. McDowell, Intermolecular spin-diffusion between  $^{31}\text{P}$  nuclei in a single crystal of dipotassium  $\alpha$ -D-glucose-1-phosphate dihydrate; a 1-D analogue of the 2-D exchange NMR experiment, *Chem. Phys. Lett.* **113**, 123-128 (1985).
18. J. Jeener, B. H. Meier, P. Bachmann, and R. R. Ernst, Investigation of exchange processes by two-dimensional NMR spectroscopy, *J. Chem. Phys.* **71**, 4546-4553 (1979).
19. Y. Yang, M. Schuster, B. Blümich, and H. W. Spiess, Dynamic magic-angle spinning NMR spectroscopy: Exchange induced spinning sidebands, *Chem. Phys. Lett.* **139**, 239-243 (1987).
20. V. Gérardy-Montouillout, C. Malveau, P. Tekely, Z. Olender, and Z. Luz, ODESSA, a new 1D-exchange experiment for chemically equivalent nuclei in rotating solids, *J. Magn. Reson. A* **123**, 7-15 (1996).
21. D. Reichert, H. Zimmermann, P. Tekely, R. Poupko, and Z. Luz, Time-reverse Odessa. A 1D Exchange experiment for rotating solids with several groups of equivalent nuclei, *J. Magn. Reson.* **125**, 245-258 (1997).
22. D. E. Favre, D. J. Schaefer, and B. F. Chmelka, Direct determination of motional correlation times by 1D MAS and 2D exchange NMR techniques, *J. Magn. Reson.* **134**, 261-279 (1998).
23. P. Tekely, J. Brondeau, K. Elbayed, A. Retournard, and D. Canet., A simple pulse train, using  $90^\circ$  hard pulses, for selective excitation in high-resolution solid-state NMR, *J. Magn. Reson.* **80**, 509-516 (1988).
24. R. G. Larsen, Y. K. Lee, B. He, J. O. Jang, Z. Luz, H. Zimmermann,

- and A. Pines, Carbon-13 chemical shift tensor correlation via spin diffusion in solid tropolone using switched-angle spinning spectroscopy, *J. Chem. Phys.* **103**, 9844–9854 (1995).
25. H. Shimanouchi and Y. Sasada, Crystal and molecular structure of tropolone, *Acta Crystallogr. B* **29**, 81–90 (1973).
26. Z. Olender, D. Reichert, A. Mueller, H. Zimmermann, R. Poupko, and Z. Luz, Carbon-13 chemical-shift correlation, spin-diffusion and self diffusion in isotopically enriched tropolone, *J. Magn. Reson. A* **120**, 31–45 (1996).
27. J. Laherrère and D. Sornette, Stretched exponential distributions in nature and economy: “fat tails” with characteristic scales, *Eur. Phys. J. B* **2**, 525–539 (1998); G. Williams and D. C. Watts, Non-symmetrical dielectric relaxation behaviour arising from a simple empirical decay function, *Trans. Faraday Soc.* **66**, 80–85 (1970).
28. P. Tekely, To what extent does the centerband and each spinning sideband contain contributions from different crystallites of the powder sample, *Solid State NMR* **14**, 33–43 (1999).
29. C. E. Bronniman, N. M. Szeverenyi, and G. E. Maciel, <sup>13</sup>C spin diffusion of adamantane, *J. Chem. Phys.* **79**, 3694–3700 (1983).